The unique molecular disorder of crystalline 4-chloro-2,6-dimethyl-3-iodopyridine *N*-oxide. An X-ray and spectroscopic study

**J. Hanuza,[a] M. Maczka,[a] A. Waskowska,[a] W. Oganowski,[a]
H. Ban-Oganowska,[b] J. H. van der Maas[c] and E. T. G. Lutz[c]**

[a] *Institute of Low Temperature and Structure Research, Polish Academy of Sciences, 50–950 Wroclaw, Poland*
[b] *Department of Organic Chemistry, Academy of Economics, Wroclaw, Poland*
[c] *Utrecht University, Faculty of Chemistry, Department of Analytical Molecular Spectrometry, The Netherlands*

The crystal structure of 4-chloro-2,6-dimethyl-3-iodopyridine *N*-oxide has been determined at ambient temperature. The compound crystallizes in monoclinic structure, space group $P2_1/n$. The asymmetric unit consists of two formula units, one of which shows positional disorder. The shortest intermolecular contacts form a medium strong hydrogen bond of the type =C–H · · · O. The IR and Raman spectra, measured in the region 50–3500 cm^{-1}, are in agreement with predictions based on the X-ray structural data. The observed electron absorption bands have been attributed to transitions between singlet levels, whereas the emission originates from transitions between the excited triplet level and the ground singlet level. The splitting of the strongest absorption band (225–242 nm) into three components has been explained to be a result of expansion of the valence shell of the iodine atom (d-orbital resonance).

Introduction

The chemistry of heterocyclic *N*-oxides has gained importance due to their interesting biological activity. These compounds exhibit antibacterial[1] and antifungal properties[2] and are prospective crystals for second-harmonic generation.[3] Vibrational spectra of pyridine *N*-oxide have been investigated previously [4–8] and matrix isolation experiments showed that upon self-association pyridine *N*-oxide molecules show splitting of some vibrational bands.[9] This splitting is observed for those modes which are very sensitive to the environment[5] and consequently are assigned to the multiple site effect.[9] Recently, Bougeard *et al.*[10] published a lattice dynamic study including low frequency Raman and infrared spectra of 4-nitropyridine *N*-oxide. A complete assignment of all vibrational modes of 2,6-dimethylpyridine has been reported by Green *et al.*[11] and Draeger.[12]

Heterocyclic *N*-oxides have also been studied with electronic absorption[13–18] and luminescence spectroscopy.[17,19–23] A strong UV band at 280 nm, observed for pyridine *N*-oxide in aprotic solvents, was assigned to the electron transition from the oxygen atom of the *N*-oxide group to the ring π-system.[14] The observed luminescence is due to either the transition from the excited triplet state to the ground singlet state (phosphorescence) or to the transition from the excited singlet state to the ground singlet state (fluorescence).[22]

The structure of the title compound has been studied spectroscopically in detail because of its unique crystal disorder together with its unexpected strong luminesence properties.

Experimental

Synthesis

2,6-Dimethyl-3-iodo-4-nitropyridine *N*-oxide (5 g) was treated with 25 ml of acetyl chloride. The reaction mixture was maintained at 50 °C for 30 min, then excess of acetyl chloride was decomposed with ice and neutralized with aqueous sodium carbonate. The reaction product was extracted with chloroform. The crude product (4.3 g, 89%) was crystallized from acetone. The pure crystals were pale yellow, mp 119–121 °C, hardly soluble in water and acetone, insoluble in diethyl ether, but readily soluble in ethanol, benzene and chloroform.

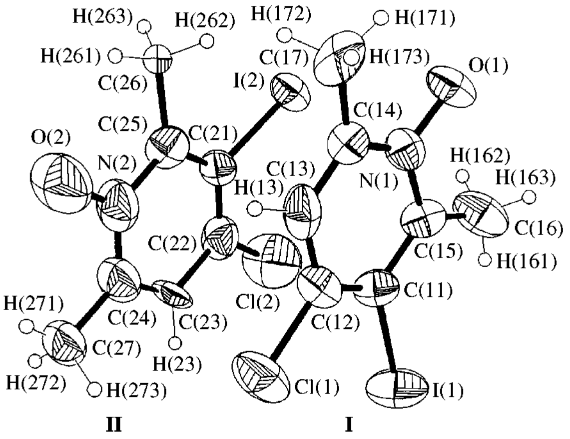

Fig. 1 The asymmetric unit showing atom numbering scheme. The displacement ellipsoids for non-H atoms are drawn at the 50% probability level.

X-Ray diffraction

Experimental and instrumental details are given in Table 1. The structure was solved by direct methods. The E-map contained two independent units consisting of well defined six-membered rings together with **I**(1) and **I**(2) atoms. Difference electron density maps based on this partial structure revealed unambiguously the remaining atoms of unit **I**, whereas there was no obvious choice for the location of the Cl(2), O(2), N(2), and C(26) atoms belonging to unit **II** (Fig.1). The same structural picture emerged from the Patterson map calculations. Several trials with different configurations led to models with abnormal thermal displacement amplitudes: high for Cl(2), N(2) and O(2) and low for the methyl carbon C(26). The peaks corresponding to the questionable atoms on the electron density map appeared to be split, pointing to 'occupational' dis-

Table 1 Experimental X-ray details

Crystal data	
Chemical formula	C_7H_7NOClI
Molecular mass	283.5
Crystal system	Monoclinic
Space group	$P2_1/n$
Lattice parameters/Å	$a = 8.901(2)$, $b = 8.875(2)$, $c = 23.152(5)$
B(°)	99.35(3)
V/Å^3	1804.4(7)
Z	8
Radiation, wavelength	Mo-Kα, 0.71073 Å
No. of reflections	30
θ range (°)	12, 15
μ/min^{-1}	3.75
T/K	294
Crystal colour and form	Colourless, plate
Crystal size	0.1 × 0.3 ×0.15 mm
D_c/Mg m^{-1}	1.951(1)
Data collection	
Diffractometer	Kuma KM-4
Absorption correction	Empirical on ψ-scan
No. of measured reflections	6178
No. of independent reflections	2746
No. of observed reflections	1898
Observation criterion	$F > 4\sigma(F_o)$
R_{int}	3.8% for all reflections
θ_{max} (°)	68
Index range	h: −10, 10; k: −10, 10; l: −26, 5
Standard reflections	2, measured every 50 reflections
Intensity variation	Negligible
Refinement	
Refinement on	F
Quantity minimized	$\Sigma w(F_o - F_c)^2$
Final R factor	0.041
wR	0.044
Weighting	$w = 1/[\sigma^2(F_o) + 0.0017F^2]$
S	1.8
No. of refined parameters	197
H-atoms	From geometry, not refined
$(\Delta/\sigma)_{max}$	0.036
$\Delta\rho_{min}$, $\Delta\rho_{max}$	− 0.46, 087

order about the axis passing through the **I**(2) and C(27) atoms. The best result of refinement with molecule **II** in one of the two possible configurations led to the conventional discrepancy factor $R = 0.068$, goodness of fit 1.34. The alternative configuration of molecule **II** after 180° rotation about the direction of the I(2)–C(27) atoms gave $R = 0.078$. These results showed that the crystal, as a whole, consists of two types of domains each of which dominates one of the two possible orientations of molecule **II**. Therefore in the final cycle of the refinement it was assumed that the double peak ascribed to Cl(2) corresponds to both the Cl(2) and C(26) atoms present with random distribution (population factor 0.5). A similar approach was made to the location of the N(2)–O(2) group in molecule **II**. The atom N(2), shown in Fig. 1, can as well occupy the position of C(23) with attached O(21). The alternative positions of these atoms are marked with non-shadowed thermal ellipsoids and empty bond sticks. The H-atoms belonging to molecule **I** were positioned on the basis of geometric considerations. They were included in the structure factor calculations, but not varied.

Atomic scattering factors for neutral atoms and correction for the anomalous dispersion were as in the SHELXTL program system[24] which was also used for all structure calculations and drawings (on an IBM PC computer).

Raman and infrared measurements

Infrared spectra were recorded on a Perkin-Elmer 2000 FT-IR spectrometer. The KBr pelleting technique was applied for spectra in the region 450–4000 cm^{-1} and the far-infrared spectrum was taken from a Nujol suspension, sandwiched between polyethene windows. Spectra of dilute solution in CCl_4 were recorded in 0.5 mm NaCl cells. A Specac P/N 21.000 variable temperature cell, equipped with KBr windows, connected to a West microprocessor-based temperature controller was used as a cryostat. The spectra were recorded as KBr pellets at 90–400 K at a reduced pressure of 120 mTorr. Cooling was realised with liquid nitrogen.

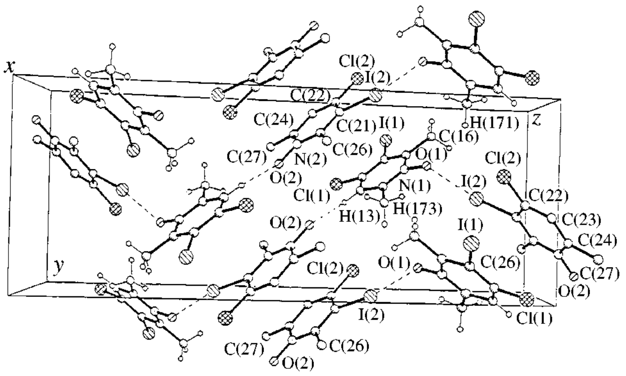

Fig. 2 The perspective view of the crystal structure

The Raman spectrum of the polycrystalline sample was measured in the back-scattering configuration with a Perkin-Elmer 2000 FT-NIR–Raman spectrometer equipped with an InGaAs detector and connected to a PC under GRAMS 386 Research software. Excitation was performed with a YAG : Nd^{3+} laser, output laser power: 100 mW. Scanning conditions for both IR and Raman spectra were: optical resolution: 2 cm^{-1} and apodization: medium.

Electron absorption and luminescence spectra

The electron absorption spectra were recorded on a Cary 2300 Varian UV–VIS–NIR spectrophotometer. Emission measurements were performed on a DFS 24 Spectrometer. The 457.9 and 488 nm lines of an Argon IKA 120 laser were used for sample excitation. The output laser power was 150 mW.

Crystal structure determination

The asymmetric unit consists of two formula units, one of which shows positional disorder. The refinement gives two comparable results with two possible configurations of molecule **II**. A comparison of the bond lengths and angles with the values of pure pyridine,[25] pyridinium iodide[26] and salts with hexa-chlorometallates[27] shows that replacement of H-atoms at the pyridine nucleus by other substituents does not distort the geometry of the ring itself. The pyridine mean C–C bond length is 1.380(12) and 1.382(12) Å in unit **I** and **II**, respectively, which is consistent with the accepted aromatic C–C bond length (1.394 Å). Planarity of the molecule can be seen from the sum of the bond angles C–C–C, C–N–C and N–C–C, which is approximately 360°. A perspective view of the molecular arrangement in the unit cell is shown in Fig. 2. A significant short intermolecular contact is recognised for the I(2) · · · O(1) contacts with a distance of 2.872(6) Å.

All interatomic contacts with distances shorter than 3.75 Å are listed in Table 2. The O(2) · · · C(13) separation could be considered as a hydrogen bond linkage with the distance 3.264(17) Å and the O(2) · · · H(13) distance of 2.374(14) Å and the contact angle O(2) · · · H(13)–C(13) equal to 153.8(6)°. The other intermolecular distances are typical van der Waals contacts between aromatic molecules.[28]

The relatively loose packing of these moieties might explain, at least partially, the structural disorder. In case of static disorder one can consider that in the unit cell molecule **II** takes one of two possible orientations, which results in the overlap model. The dynamic effect would be connected with the thermal

Table 2 Intermolecular distances shorter than 3.75 Å

A···B	Distance/Å
I(2)···O(1)$_i$	2.872(6)
Cl(1)···C(23)	3.714(11)
Cl(1)···C(24)	3.514(11)
Cl(1)···C(27)	3.625(13)
Cl(1)$_{ii}$···C(27)	3.539(11)
Cl(2)···C(16)$_i$	3.621(12)
O(2)···C(13)$_{iii}$	3.264(17)

Symmetry codes: *i*, $\frac{1}{2} - x, y - \frac{1}{2}, \frac{1}{2} - z$; *ii*, $-x, 1 - y, 1 - z$; *iii*, $1 - x, 1 - y, 1 - z$.

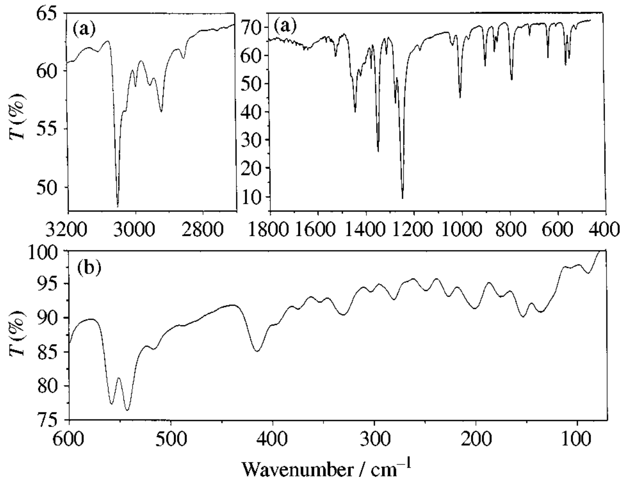

Fig. 3 Mid-IR (a) and far-IR (b) spectra of polycrystalline 4-chloro-2,6-dimethyl-3-iodopyridine *N*-oxide

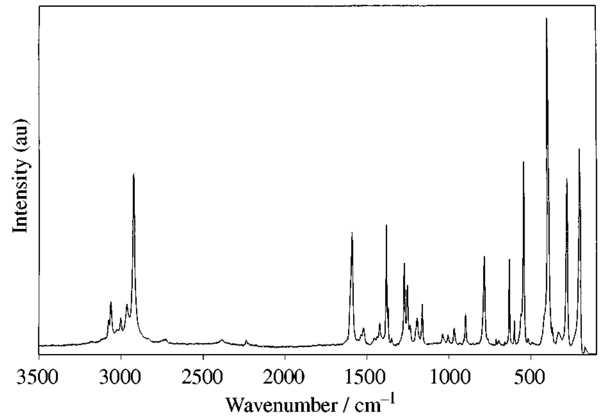

Fig. 4 Raman spectrum of polycrystalline 4-chloro-2,6-dimethyl-3-iodopyridine *N*-oxide

Table 3 Vibrational frequencies (ν/cm^{-1}) for 4-chloro-2,6-dimethyl-3-iodopyridine *N*-oxide

Raman	IR crystal	IR soln.	Assignment
3074w		3076w	ν(=C–H)
3059w	3052w		ν(=C–H)
3020w	3025m		
3000w	2996w	3000w	$\nu_{as}(CH_3)$
2961w	2953w	2961w	$\nu_{as}(CH_3)$
2921s	2919w	2925m	$\nu_s(CH_3)$
	2855w		$\nu_{as}(CH_3)$ overtone
1599sh			
1589m			ν_{8a} ring stretch
1532w			
1517w	1517w	1519w	ν_{8b} ring stretch
1456w	1451sh		ν_{19b} ring stretch
1437w	1439m	1440m	$\delta_{as}(CH_3)$
1417w	1415w	1419w	ν_{19a} ring stretch
1380m	1389sh	1386w	$\delta_s(CH_3)$
1383m	1382sh		$\delta_s(CH_3)$
1369w	1371w	1375w	$\delta_s(CH_3)$
1348w	1346s	1347vs	ν_{14} in-plane ring bend
	1306w	1308w	
1271m	1271w	1274s	
	1250m		
1252m	1231s	1258vs	ν(N–O)
	1238m		
1192w			
1168w	1167w		δ(C–H)
1161w		1162w	δ(C–H)
1037w	1037sh	1036w	CH_3 rocking
	1031w		CH_3 rocking
1003w	1001m	1001m	ν_{12} in-plane ring bend
966w	962w	964w	$\nu(C-CH_3)$
898w	896w	900w	CH_3 rocking
	857w	862w	γ(C–H)
	846w		γ(C–H)
784m	785m		ν_1 ring stretch
	708w		ν_4 out-of-plane ring deformation
632m	632m		ν_{6b} in-plane ring deformation
598w	597vw		
557sh	559m		ν_{16b} out-of-plane ring deformation
544s	543m		ν_{6a} in-plane ring deformation
518w	514w		δ(N–O)
412sh	415w		ν_{16a} out-of-plane ring deformation
397vs	400sh		ν(C–Cl)
375sh	373w		$\delta(C-CH_3)$
	352w		
331w	330w		γ(N–O)
279s	280w		δ(C–Cl)
	246w		$\gamma(C-CH_3)$
	226w		$\gamma(C-CH_3)$
202m	200w		ν(C–I)
	174w		γ(C–Cl)
	154w		δ(C–I)
	135w		γ(C–I)
	88w		translational or librational mode

motions about the axis passing through the I(2)–C(27) atoms. Since in this structure there is not enough space for a 180° librational rotation, it seems more justified to consider the observed disorder as a static effect, exerted by stacking disorder.

Atomic coordinates, thermal parameters, and bond lengths and angles have been deposited at the Cambridge Crystallographic Data Centre (CCDC). See 'Instructions for Authors', *J. Chem. Soc., Perkin Trans. 2*, 1997, Issue 1. Any request to see the CCDC for this materal should quote the full literature citation and the reference number 188/79.

Vibrational characteristics

The unit-cell of 4-chloro-2,6-dimethyl-3-iodopyridine *N*-oxide (ClDMIPNO) consists of eight molecules giving rise to 429 zone centre modes of which 384 are internal, 24 librational, 21 translational and 3 acoustic. The vibrational frequencies of all these modes could be established only from polarized IR and Raman spectra of a single crystal. The relatively loose packing of the molecules in the crystal lattice indicates that most intermolecular interactions are weak, except the C–H···O and C–I···O contacts. Therefore, the spectra of the polycrystalline sample can be well described by taking into consideration the vibrations of the single molecule only and the observed splitting of some modes can be explained as a result of two non-equivalent crystallographic sites.

We have chosen to consider the vibrations of the substituted pyridine ring separately from those of the methyl substituents. There are 48 modes for a single molecule of ClDMIPNO. Eighteen of them describe the methyl group vibrations. Because the title molecule has C_s symmetry, 30 vibrations of the substituted pyridine ring can be described by 21A′ + 9A″ irreducible representations. The (mid and far) IR and Raman spectra are presented in Figs. 3 and 4. A listing of the observed bands and assignment have been presented in Table 3.

For the single pyridine ring hydrogen atom of an isolated molecule three different vibrations are expected, *e.g.* =C−H stretch, in plane bend and out-of-plane deformation. The crystal data have shown that there are two different types of =C−H bonds in the crystal. Hydrogen atom H(13) of unit **I** interacts with the oxygen atom O(2) of unit **II** while H(23) has no short intermolecular contact. The existence of the C−H · · · O hydrogen bonds has been and still is the subject of much debate.[29,30] Crystallographers usually base their hydrogen bonding arguments on the existence of H · · · O distances smaller than the sum of the van der Waals radii (2.4–2.7 Å). In this crystal the H · · · O distance is 2.374(14) Å and thus this C−H · · · O interaction could be regarded as a hydrogen bond. With reference to Bougeard *et al.*[10] we suggest that these specific interactions play an important role in crystal packing.[28,30,31] Previously we reported[29,32,33] that interaction between a C−H and an oxygen atom results in a red shift for the C−H stretching band and a blue shift for the =C−H bending vibration if compared to the position of the free C−H group.

In the present study, the =C−H stretch band is split into two components in the Raman spectrum, at 3066 and 3054 cm^{-1}, while the IR spectrum shows just one band at 3052 cm^{-1}. Consequently the band at 3066 cm^{-1} is assigned to the C(23)−H stretching vibration. The 3054–3052 cm^{-1} band, assigned to the C(13)−H stretch, is red shifted in comparison to the C(23)−H stretch, due to the =C−H · · · O interaction. The more intense C(13)−H stretching band obscures the weak band of the C(23)−H stretching mode in IR. The existence of the C−H · · · O hydrogen bonding in the crystal structure is also confirmed by the splitting of the C−H in-plane bending and the C−H out-of-plane stretching vibrations into two components. These pairs of modes are observed at 1168, 1161 and 857, 846 cm^{-1}, respectively.

The strongest band in the IR spectrum is observed at 1231 cm^{-1} together with adjacent absorptions at 1238 and 1250 cm^{-1}; and the Raman band at 1252 cm^{-1} these are assigned to the N−O stretch, because this vibration is accompanied by a large change in dipole moment and polarizability. The blue shifted very strong IR band at 1258 cm^{-1} supports both the assignment to ν(N−O) and the existence of C−H · · · O−N hydrogen bonding.

Since ClDMIPNO is a planar molecule and has one conformer only, the splitting of the N−O vibration can be interpreted as a result of intermolecular interaction in the crystal lattice. As has been shown, the oxygen atoms O(2) of the molecules **II** interact with the hydrogen atoms H(13) of the molecules **I**. On the other hand, the oxygen atom O(1) of the unit **I** molecules interacts with the iodide atom I(2) of the unit **II** molecule. The two N−O distances in the ClDMIPNO crystal are 1.316 and 1.336 Å. The splitting of the N−O stretching vibrations was previously observed in a solid state spectrum of pyridine *N*-oxide[9] and 2,6-dimethylpyridine *N*-oxide.[34] Accordingly we also expected to observe a similar splitting in the case of the in-plane N−O bending and the out-of-plane N−O deformation modes. These N−O modes were observed with medium to strong intensity in IR and Raman spectra at 482 and 465 cm^{-1} for 4-chloro- and 4-nitro-pyridine *N*-oxide[35] and 469 cm^{-1} for pyridine *N*-oxide.[9]

The vibrational spectra of ClDMIPNO shows three bands in the 514–559 cm^{-1} region. In comparison with other pyridine derivatives the weak bands at 518–514 cm^{-1} are assigned to the δ(N−O) vibration. The remaining two bands at 557–559 and 544–543 cm^{-1} could be assigned to the ν_{16b} and ν_{6a} vibrations. Previous studies have shown that in-plane ring deformation modes are observed as strong bands in Raman and IR spectra. These modes were observed at 556, 548 and 542 cm^{-1} for 2,6-dimethylpyridine, 3,5-dimethylpyridine[14] and pyridine *N*-oxide.[9] Accordingly, the strong Raman and medium intensity IR bands at 544–543 cm^{-1} have been assigned to ν_{16b} and those at 559–557 to ν_{6a} vibrations. No splitting was observed for the γ(N−O) mode (331–330 cm^{-1}).

The crystallographic data show that the two molecules are also in contact due to the short I(2) · · · O(1)$_i$ distance of 2.872(6) Å. However, the interaction of the I(2) atom with the oxygen atom does not change considerably the C−I bond length. The C(11)−I(1) bond length of molecule **I** is 2.093 Å and C(21)−I(2) of molecule in unit **II** is 2.095 Å. Hence, the C−I stretching and bending modes are expected as singlets, which is in accordance with observations.

The splitting of the symmetric deformation mode of the methyl groups into a doublet at 1382–1389 cm^{-1} and a single peak at 1371 cm^{-1} yields spectroscopic evidence for two non-equivalent sites in the crystal. In CCl_4 solution the two chemically different methyl groups show a doublet at 1386 and 1375 cm^{-1}. As has been shown by Green *et al.*[11] CH_3 symmetric deformation modes are sensitive to environmental changes. Two bands were observed for 2,3-dimethylpyridine: 1384 and 1369 cm^{-1}.[36]

For the remaining bands no splitting due to crystal packing could be recognised. The ring stretching vibrations ν_{8a} and ν_{8b} were observed at 1589 and 1517 cm^{-1}. The frequency difference between these two vibrations is strongly increased if an oxygen atom is attached to the pyridine ring. The respective values are 1583/1572 cm^{-1} for pyridine,[37] 1591/1578 cm^{-1} for 2,6-dimethylpyridine[14] and 1606/1554 cm^{-1} for pyridine *N*-oxide.[9] It is difficult to distinguish the CH_3 rocking, in-plane ring bending (ν_{12}) and the ring stretching (ν_1) vibrations. The ν_1 vibration is observed as a very strong band in the Raman spectrum and a medium intensity one in the IR spectrum at 996 cm^{-1} for 2,6-dimethylpyridine.[14] However, this mode is very sensitive to electronegative substitution and is observed at 836 cm^{-1} for pyridine *N*-oxide[9] and 876 cm^{-1} for 4-nitropyridine *N*-oxide.[38] Accordingly, the medium intensity bands at 787 cm^{-1} (Raman) and 785 cm^{-1} (IR) have been assigned to the ν_1 vibration. The remaining singlet at 1001 cm^{-1} and doublet at 1031/1037 cm^{-1} originate from the in-plane ring bending (ν_{12}) and CH_3 rocking vibrations, respectively.

The pyridine ring–halogen stretching and in-plane bending vibrations give rise to strong Raman and weak IR bands.[35,39,40] Therefore, the very strong Raman band at 395 cm^{-1} originates from the ring–chlorine stretching vibration. This band was observed at 384 cm^{-1} for 4-chloropyridine *N*-oxide[35] and 428 cm^{-1} for 3-chloropyridine.[40] The second strong band was observed at 279 cm^{-1}, and is caused by the in-plane ring–chlorine bending vibration, located at 280 cm^{-1} for 4-chloropyridine *N*-oxide[35] and 294 cm^{-1} for 3-chloropyridine.[40] The third strong band at 200 cm^{-1} originates from the ring–iodide stretching vibration. Former studies on halopyridines showed that the frequency of the stretching and bending vibration depends on the atomic mass of the substituent.[39,40] A frequency decrease from fluoride to iodide has been reported. The ring–iodide stretching modes were located at 259 and 263 cm^{-1} for 2- and 3-iodopyridine.[40] The bands below 200 cm^{-1} cannot be assigned with a high degree of certainty. These originate most likely from the in-plane ring–iodide deformation, out-of-plane ring–halogen atom deformations, translations, librations and possibly lattice vibrations.

Electronic properties

The electronic structures and spectra of heterocyclic amine *N*-oxides have been extensively studied by many researchers.[16–21] In the case of pyridine *N*-oxide, the strong $\pi \longrightarrow \pi^*$ band was observed near 280 nm, in aprotic solvents. This band has $^1A_1$ symmetry and it has the largest contribution of the intramolecular charge transfer configuration due to the electron transition from the *N*-oxide oxygen atom to the ring π-system. On going from pyridine *N*-oxide to 2,6-dimethylpyridine *N*-oxide this band shows a blue shift to 274 nm.[41] The study of 3-halo-2,6-dimethylpyridine *N*-oxides has shown that apart from the strong 272–278 nm band, two or

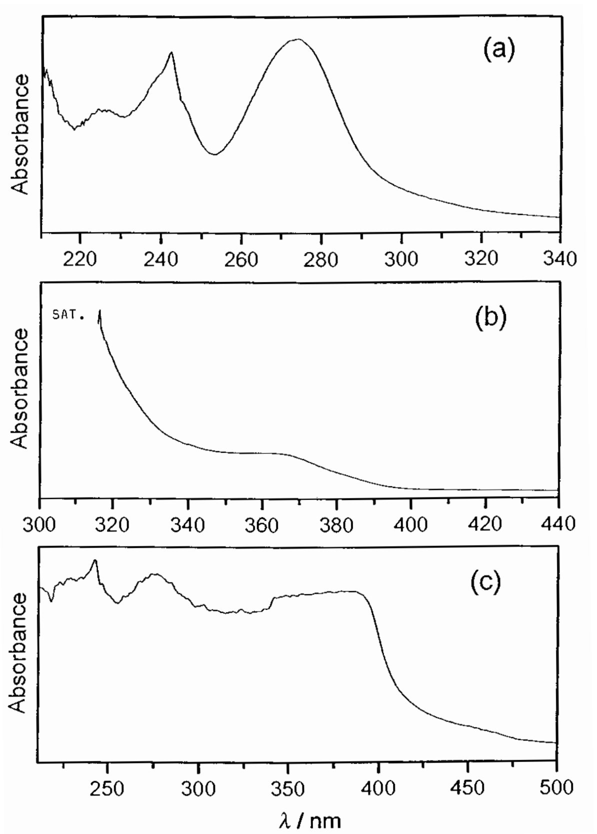

Fig. 5 Electron absorption spectra of 4-chloro-2,6-dimethyl-3-iodopyridine *N*-oxide in the methanol solution (a and b) and single crystal (c)

Table 4 Absorption bands for 4-chloro-2,6-dimethyl-3-iodopyridine *N*-oxide

Polycrystalline, λ/nm	CH_3OH solution, λ/nm	Assignment
385.7 s	363.3 vw	$n \longrightarrow \pi^*$ or intermolecular CT transition
275.6 m	273.5 s	$\pi \longrightarrow \pi^*$
242.1 m	242.1 s	$\pi \longrightarrow \pi^*$
	239.4 sh	$\pi \longrightarrow \pi^*$
226.1 w	225.4 w	$\pi \longrightarrow \pi^*$

three more bands are observed in the regions 220–240 and 310–330 nm.[42,43]

The electron absorption spectrum of 4-chloro-2,6-dimethyl-3-iodopyridine in methanol solution (Fig. 5, Table 4) is very similar to that of 2,6-dimethyl-3-iodopyridine.[42] The strongest band, assigned to the $\pi \longrightarrow \pi^*$ transition, is observed at 273.5 nm and is red-shifted by 4.5 nm in comparison to 3-iodo-2,6-dimethylpyridine. The band, assigned to the excitation of an electron from a skeletal carbon–carbon double bond to a level with uniform charge distribution over the molecule,[43,44] is split into the three components, observed at 242.1, 239.4 and 225.4 nm. The respective transitions for 3-iodo-2,6-dimethylpyridine were located at shorter wavelengths: 236, 221 and 210 nm, respectively. The splitting of this band into three components is due to the expansion of the valence shell of iodide atom (d-orbital resonance).[45,46]

The third, weak band is observed at 363.3 nm. It might originate from the $n \longrightarrow \pi^*$ transition, *i.e.* excitation from the HOMO to either the LUMO or the next MO.[45] This band is observed at a significantly higher energy (363.3 nm) for 4-chloro-2,6-dimethyl-3-iodopyridine *N*-oxide than for 3-iodo-2,6-dimethylpyridine *N*-oxide (329 nm). The solid-state spectrum differs from that in methanol solution mainly due to the red shift and intensity increase of the third band (Table 4). So a significant intensity increase may indicate that this band might be assigned to the intermolecular charge transfer transition rather than to the $n \longrightarrow \pi^*$ transition. The positions of the bands remain fairly constant; experimentally a shift of only a few nm is observed.

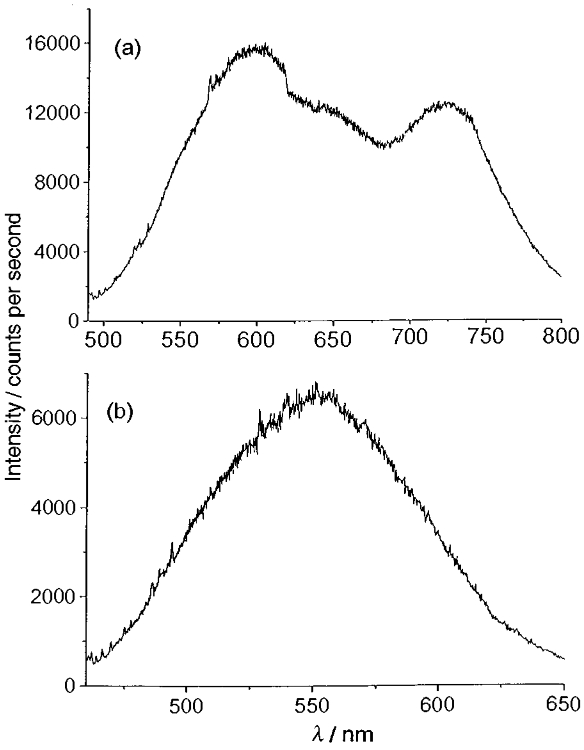

Fig. 6 Luminescence spectra of 4-chloro-2,6-dimethyl-3-iodopyridine *N*-oxide recorded with 488 nm (a) and 457.9 nm (b) laser line excitation

Luminescence spectra

The electronic properties of the pyridine *N*-oxide derivatives have been studied mainly by UV absorption spectroscopy. Very few luminescence studies have been reported since most heterocyclic amine *N*-oxides are not luminescent or their luminescence spectra are more or less contaminated by emission of unexpected products of photochemical reactions.[17] Luminescence studies have been reported for pyridine *N*-oxide,[20] 2-pyridone[21] and for a number of nitro aromatic compounds.[17,22,23] The observed luminescence of pyridine *N*-oxide was due to electronic transitions between the excited singlet states and the ground singlet state. All observed bands were located below 350 nm.[20] Nitro aromatic compounds exhibit either fluorescence (*i.e.* transition from the excited singlet state) or phosphorescence (*i.e.* transition from the excited triplet state). It was concluded that nitro compounds, in which the aromatic part is small, exhibit only phosphorescence due to the transition from the $^3\pi,\pi^*$ triplet state to the ground singlet state.[22] This broad-band phosphorescence falls in the region 500–800 nm.

In the present study the luminescence spectrum shows four bands when the sample is illuminated at 488 nm (600, 623, 644 and 723 nm) and only one broad band at 550 nm for 457.9 nm excitation (Fig. 6). In the former studies the two bands were observed for 4-nitropyridine *N*-oxide solution in diethyl ether at 578.5 and 613.5 nm but when isopropyl alcohol was added to the ethereal solution a third band, caused by the hydrogen bonding interaction, appeared at 550 nm.[17] Later studies confirmed that the 550 nm band originates from the hydrogen-bonding complexes, and when a very strong hydrogen-bonding complex is formed, as in the case of 4-nitropyridine *N*-oxide in 2,2,2-trifluoroethanol matrix, only broad and structureless phosphorescence is observed.[23] In the ClDMIPNO crystal, hydrogen-bonding is present between the *N*-oxide oxygen atom of a unit **II** molecule and a hydrogen atom of molecule **I**. Therefore, we assign the broad and strong band at 550–600 nm to the hydrogen-bonded complex phosphorescence. The remaining bands, observed at 623, 644 and 723 nm for 488 nm excitation only, might be assigned to phosphorescence of unit **I** for which the oxygen atom interacts with the iodide atom of molecule **II**. Such a large energy difference between the hydrogen-bonded complex and non-bonded molecule is unexpected; most likely these bands arise from some photochemical decomposition product.

Conclusions

An unusual disorder in the crystal structure of the title compound has been established by X-ray and vibrational spectroscopy. Doublet splitting of vibrational modes assigned to N−O, =C−H and CH_3 functionalities is in agreement with predicted intermolecular interactions in the crystal. With the exclusion of the splitting phenomena the number of observed vibrational modes is in nice agreement with predictions based on the isolated molecule. The electron absorption spectrum consists of two singlets at 363–386, 273–276 nm and one triplet at 242.1, 239.4 and *ca.* 226 nm. These bands originate from transitions between the ground singlet level and the different excited singlet levels. Emission bands are due to transitions between the excited triplet level and the ground singlet level.

References

1 R. E. Muntwyler, *Ger. Offen.*, 2,714,41, 13 Oct., 1977.
2 H. L. Plant and A. R. Bell, *U.S. Patent* 3,390,542, 1 Jan., 1976.
3 D. Josse, R. Hierle, I. Ledoux and J. Zyss, *Appl. Phys. Lett.*, 1988, **53**, 2251.
4 P. Mirone and B. Fortunato, *Atti Accad. Nazl. Lincei, Rend., Classe Sci. Fis., Mat. Nat.*, 1963, **34**, 168.
5 P. Mirone, *Atti Accad. Nazl. Lincei, Rend., Classe Sci. Fis., Mat. Nat.*, 1963, **35**, 530.
6 G. Varsanyi, S. Szoke, G. Keresztury and A. Galleri, *Acta Chim. Acad. Sci. Hung.*, 1970, **65**, 73.
7 V. I. Berezin, *Optika Spektrosk.*, 1965, **18**, 212.
8 Y. Kakiuti, H. Saito and M. Akiyama, *J. Mol. Spectrosc.*, 1970, **35**, 66.
9 Z. Mielke, *Spectrochim. Acta, Sect. A*, 1983, **39**, 141.
10 D. Bougeard, J. R. Burie, Nguyen Quy Dao and B. Hennion, *Spectrochim. Acta*, 1995, **51*A***, 21.
11 J. H. S. Green, D. J. Harrison, W. Kynaston and H. P. Paisley, *Spectrochim. Acta, Sect. A*, 1970, **26**, 2139.
12 J. A. Draeger, *Spectrochim. Acta, Sect. A*, 1983, **39**, 809.
13 N. Mataga and T. Kubota, *Molecular Interactions and Electronic Spectra*, Marcel Dekker, New York, 1970.
14 H. Miyazaki, T. Kubota and M. Yamakawa, *Bull. Chem. Soc. Jpn*, 1972, **45**, 780.
15 M. Yamakawa, T. Kubota and H. Akazawa, *Theor. Chim. Acta*, 1963, **15**, 244.
16 K. Seibold, G. Wagniera and H. Lebhart, *Helv. Chim. Acta*, 1969, **52**, 789.
17 M. Yamakawa, T. Kubota, K. Ezumi and Y. Mizuno, *Spectrochim. Acta, Sect. A*, 1974, **30**, 2103.
18 E. Ochiai, *Aromatic Amine Oxides*, Elsevier, Amsterdam, 1967.
19 S. Knuts, H. Agren and B.F. Minaev, *Theochem.*, 1994, **117**, 185.
20 Y. Nakagawa, I. Suxuka and M. Ito, *Chem. Phys. Lett.*, 1993, **208**, 453.
21 A. C. Testa, *J. Photochem. Photobiol.*, 1992, **A64**, 73.
22 O. S. Khalil, H. G. Bach and S. P. McGlynn, *J. Mol. Spectrosc.*, 1970, **35**, 455.
23 T. Ehara, A. Akiyama, T. Ikoma, Y. Ikegami and S. Tero-Kubota, *J. Phys. Chem.*, 1995, **99**, 2292.
24 G. M. Sheldrick: SHELXTL-PLUS. Siemens Analytical Instruments, Madison, Wisconsin, USA, 1990.
25 B. Bak, L. Hansen-Nygaard and J. Rastrup-Andersen, *J. Mol. Spectrosc.*, 1958, **2**, 316.
26 H. Hartl, *Acta Crystallogr., Sect. B*, 1975, **31**, 1781.
27 D. Borchers and A. Weiss, *Z. Naturforsch. Teil A*, 1987, **42**, 739.
28 G. R. Freeman and C. E. Bugg, *Acta Crystallogr., Sect. B*, 1974, **30**, 431.
29 E. Steinwender, E. T. G. Lutz, J. H.van der Maas and J. A. Kanters, *Vib. Spectrosc.*, 1993, **4**, 217.
30 R. Taylor and O. Kennard, *J. Am. Chem. Soc.*, 1982, **104**, 5063.
31 Z. Berkovitch-Yellin and L. Leiserowitz, *Acta Crystallogr., Sect. B*, 1984, **40**, 159.
32 B. Lutz, J. H. van der Maas and J. A. Kanters, *J. Mol. Struct.*, 1994, **325**, 203.
33 B. T. G. Lutz, J. Jacob and J. H. van der Maas, *Vib. Spectrosc.*, 1996, **12**, 197.
34 S. P. Ponomarenko, T. K. Nikolaenko and Yu. Ya. Borivikov, *Ukr. Khim. Zh.*, 1990, **56(1)**, 56.
35 M. M. Abo Aly and S. Morsi, *Spectrochim. Acta, Sect. A*, 1992, **48**, 615.
36 J. H. S. Green, *Spectrochim. Acta, Sect. A*, 1970, **26**, 1913.
37 L. Harsanyi and F. Kilar, *J. Mol. Struct.*, 1980, **65**, 141.
38 M. Joyeux and N. Quy Dao, *Spectrochim. Acta, Sect. A*, 1988, **44**, 1447.
39 K. Tanaka, K. Kassasaku, H. Shimada and R. Shimada, *Bull. Chem. Soc. Jpn.*, 1988, **61**, 1917.
40 H. Abdel-Shafy, H. Perlmutter and H. Kimmel, *J. Mol. Struct.*, 1977, **42**, 37.
41 D. Dal Monte, A. Mangini and F. Montanari, *Gazz. Chim. Ital.*, 1958, **88**, 1035.
42 H. Ban-Oganowska, *Spectrochim. Acta, Sect. A*, 1994, **50**, 1007.
43 H. Ban-Oganowska, *Pol. J. Chem.*, in press.
44 T. Kubota, *Bull. Chem. Soc. Jpn.*, 1962, **35**, 946.
45 F. M. Beringer and I. Lillien, *J. Am. Chem. Soc.*, 1960, **82**, 5135.
46 T. M. Dunn and T. Iredale, *J. Chem. Soc.*, 1950, 1181.

Paper 7/01190C
Received 19*th February* 1997
Accepted 19*th May* 1997